10. V. I. Klyatskin, Statistical Description of Dynamical Systems with Fluctuating Parameters [in Russian], Nauka, Moscow (1975).
11. V. I. Klyatskin, Stochastic Equations and Waves in Randomly Inhomogeneous Media [in Russian], Nauka, Moscow (1980).

MATHEMATICAL MODELING OF COMBINED HEAT TRANSFER IN DISPERSED MATERIALS

O. M. Alifanov, B. P. Gerasimov, T. G. Elizarova, V. K. Zantsev, B. N. Chetverushkin, and E. V. Shil'nikov

UDC 517.9:956.2/3

We show that combined heat transfer in a dispersed medium can be modeled numerically by treating convective and radiative—conductive heat transfer separately. We refine the radiative heat-transfer model by comparison with experiment.

In the develoment of a thermal shield of various technical system and aggregates of dispersed materials, it is necessary to study their thermal insulation properties in detail. The heat-transport mechanism in such materials is rather complicated, and includes heat transport directly as a result of the thermal conductivity of the material (conductive heat transport) and heat transport by radiation (radiative heat transport). If the porous medium is filled with gas, there may also be convective heat transfer. A purely experimental study of heat-transport processes and the resulting heat fluxes is difficult, and, therefore, a simultaneous study by full-scale and numerical experiments can give good results [1, 2].

In the present article we consider the methodical aspects of the mathematical modeling of combined heat transfer in a dispersed material based on optically transparent dispersed silicic materials with a 90% and more porosity of the sample used. The samples were rectangular parallelepipeds. It is required to determine the temperature of the lower surface of the sample for a specified time dependence of the temperature of its upper surface.

A general formulation of this problem includes the combined consideration of the system of equations describing radiative transport (taking account of absorption, emission, and scattering) and the laws of conservation of energy and momentum in the gas. The purpose of the study is to construct a mathematical model, to ascertain the role of each heat-transfer mechanism, to compare various methods of calculation, and to develop the optimal approach to the solution of the problem. As the most reasonable and technically relatively simply realizable approach we propose a procedure based on the separate treatment of convective and radiative—conductive heat transfer.

1. Investigation of Convective Heat Transport in a Porous Medium. We describe the nonlinear filtration of a liquid in a porous medium by the Navier—Stokes equations, which in the Boussinesq approximation, taking account of Darcy's law, we write in the following form [3]:

$$\frac{\partial \bar{\mathbf{V}}}{\partial t} + (\bar{\mathbf{V}}\nabla)\,\bar{\mathbf{V}} = -\frac{1}{\rho}\nabla P + \nu\Delta\bar{\mathbf{V}} + \beta\bar{g}T - K\bar{\mathbf{V}}, \tag{1}$$

$$\frac{\partial T}{\partial t} + (\bar{\mathbf{V}}\nabla)\,T = \chi\Delta T, \tag{2}$$

$$\nabla\bar{\mathbf{V}} = 0, \tag{3}$$

where $K = \nu\delta_{ij}/C_{\Phi i}$, $C_{\Phi i} = k_{\Phi i}\nu/g$ is the penetrability, which characterizes the geometrical properties of the porous medium, cm²; the value of $C_{\Phi i}$ does not depend on the kind of filter-

M. V. Keldysh Institute of Applied Mathematics, Academy of Sciences of the USSR, Moscow.
Translated from Inzhenerno-Fizicheskii Zhurnal, Vol. 49, No. 5, pp. 781-791, November, 1985. Original article submitted December 21, 1984.

 0022-0841/85/4905-1306$09.50

ing liquid; $k_{\Phi i}$ is the permeability, cm/sec. We introduce the following dimensionless quantities which we denote by a tilde over the letter:

$$T = \tilde{T}\frac{\nu^2}{\beta g H^3}, \quad y = \tilde{y}H, \quad x = \tilde{x}H, \quad t = \tilde{t}\,\frac{H^2}{\nu}, \quad K = \tilde{K}\,\frac{\nu}{H^2}.$$

In solving the Navier–Stokes equations in two-dimensional geometry for an incompressible liquid or gas it is generally convenient to introduce as new variables the curl of the velocity $\omega = \text{curl}\,\bar{V}$ and the stream function $\psi(V_x = \partial\psi/\partial y,\ V_y = -\partial\psi/\partial x)$. Then $\omega = \tilde{\omega}\nu/H^2$, $\psi = \tilde{\psi}\nu$, and, omitting the tilde over dimensionless quantities, Eq. (1) becomes

$$\frac{\partial\omega}{\partial t} + \frac{\partial}{\partial x}\left(\frac{\partial\psi}{\partial y}\,\omega\right) - \frac{\partial}{\partial y}\left(\frac{\partial\psi}{\partial x}\,\omega\right) = \Delta\omega + K_x\frac{\partial^2\psi}{\partial y^2} + K_y\,\frac{\partial^2\psi}{\partial x^2} + \frac{\partial T}{\partial x}. \tag{4}$$

This equation is inconvenient for a numerical solution, however, since in using an implicit longitudinal–transverse scheme [4] the presence of second derivatives of the stream function on the right-hand side imposes rigid constraints on the time step τ. In view of this, we write Eq. (4) for $K_y > K_x$ in the form

$$\frac{\partial\omega}{\partial t} + \frac{\partial}{\partial x}\left(\frac{\partial\psi}{\partial y}\,\omega\right) - \frac{\partial}{\partial y}\left(\frac{\partial\psi}{\partial x}\,\omega\right) = \Delta\omega - K_y\omega + (K_x - K_y)\,\frac{\partial^2\psi}{\partial y^2} + \frac{\partial T}{\partial x}, \tag{5}$$

and approximate Eq. (5) in the following way:

$$\begin{aligned} &\frac{\bar{\omega} - \omega}{\tau/2} + L_x(\psi,\ \bar{\omega}) + L_y(\psi,\ \omega) = \bar{\omega}_{\bar{x}x} + \omega_{\bar{y}y} - K_y\,\bar{\omega} + (K_x - K_y)\,\psi_{\bar{y}y} + T^0_{\bar{x}},\\ &\frac{\hat{\omega} - \bar{\omega}}{\tau/2} + L_x(\psi,\ \bar{\omega}) + L_y(\psi,\ \hat{\omega}) = \bar{\omega}_{\bar{x}x} + \hat{\omega}_{\bar{y}y} - K_y\hat{\omega} + (K_x - K_y)\,\psi_{\bar{y}y} + T^0_{\bar{x}}. \end{aligned} \tag{6}$$

This method of solving the Navier–Stokes equations, taking account of Darcy's law of filtration, does not impose additional constraints on the step τ for any values of K_x and K_y.

We consider problem (1)-(3) in a closed cavity of rectangular cross section. The upper wall is maintained at a constant temperature $T_0 = 1500°K$, the lateral walls are thermally insulated ($\partial T/\partial n = 0$, $x = x_0$, $x = x_N$), and a boundary condition of the third kind $\partial T/\partial n = \alpha T$, with $\alpha = 0.5$, is specified on the lower face $y = y_0$. The acceleration makes an angle of 45° with a lateral wall, which ensures the development of thermal convection (here $g = 3\cdot 9.8$ m/sec^2). The density $\rho = 1.29\cdot 10^{-3}$ g/cm^3.

The numerical calculations were performed by an implicit longitudinal – transverse difference scheme using boundary conditions taken from [4], with the exception of the equation for ω which was solved by scheme (6) without imposing additional constraints on the time step. In the region $\tilde{L} = 2$, $\tilde{H} = 1$, the problem was solved on a space net with 21 nodes in each direction. $\tilde{T}_0 = 2\cdot 10^7$, Pr = 1. Figure 1 shows the results of caclualtions for anisotropic filtration ($K_x = 5\cdot 10^5$, $K_y = 5\cdot 10^7$) corresponding to the sample studied. It is clear that the temperature distribution is determined solely by the thermal conduction, and does not depend on the structure of the flow. Such a situation is not typical for all cases. For example, calculations show that with an increase in the permeability ($K_x \sim K_y = 10^4$) the contribution of the convective component of the heat transfer is appreciable.

Thus, under the conditions considered, defined by the anisotropic permeability tensor ($K_x = 10^4$-10^6, $K_y = 10^6$-10^8), we can restrict ourselves to taking account of only radiative–conductive heat transfer in constructing a mathematical model.

2. <u>Radiative–Conductive Heat Transfer</u>. To describe the transport of radiation inside a sample it is necessary to take account of the dependence of the optical coefficients of the material on frequency, temperature, and density, and to solve the problem in three-dimensional space. All this makes the mathematical model very complicated for numerical calculation. At the same time, studies showed that this complicated formulation is largely unjustified in view of the lack of detailed information on the optical and thermophysical properties of a dispersed medium. The data in the literature on dispersed materials is essentially not systematized.

In order to construct an effective mathematical model of the phenomenon under study, we used the general methodology of a numerical experiment [1, 5]. We studied the problem of radiative–conductive heat transfer in two formulations. In the first formulation we took account of radiative heat transfer by solving the radiative transport equation directly and, in

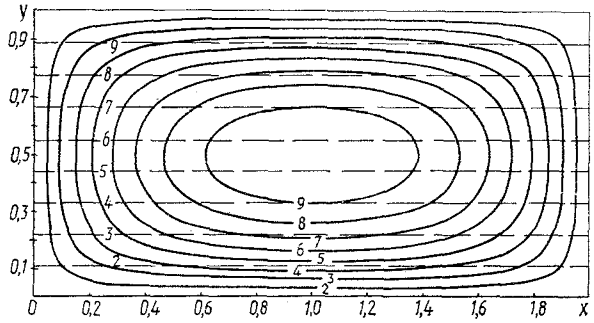

Fig. 1. Isolines of the stream function and temperature in the problem of convective–conductive heat transfer: the solid curves are streamlines: $\psi_2 = -0.0323$, $\psi_3 = -0.0246$, $\psi_4 = -0.0169$; $\psi_5 = -0.00922$, $\psi_6 = -0.00153$, $\psi_7 = 0.00616$, $\psi_8 = 0.0139$, $\psi_9 = 0.216$, $\psi_{10} = 0.0292$; the dashed lines are isotherms: $T_2 = 1.40 \cdot 10^7$, $T_3 = 1.47 \cdot 10^7$, $T_4 = 1.55 \cdot 10^7$, $T_5 = 1.62 \cdot 10^7$, $T_6 = 1.70 \cdot 10^7$, $T_7 = 1.77 \cdot 10^7$, $T_8 = 1.85 \cdot 10^7$, $T_9 = 2.00 \cdot 10^7$. All quantities are dimensionless.

the second formulation we used the radiative heat conduction approximation. The second method considerably simplifies the computational process, and makes it relatively easy to solve the problem in a two-dimensional formulation. The computational procedure within the framework of the first approach is more complicated, and the problem was solved in a one-dimensional formulation.

To a large degree the one-dimensional formulation was confirmed by the conditions of a full-scale experiment. In addition to simplifying the numerical solution, it makes it relatively easy to investigate the effect of various factors on radiative heat transfer.

1°. We write the system of equations for conductive–radiative heat transport:

$$\mu \frac{\partial I_\nu}{\partial x} + \varkappa_\nu I_\nu = \frac{\varkappa_{s\nu}}{2} \int_{-1}^{1} I_\nu g_\nu(\mu, \mu')\, d\mu' + \varkappa_{a\nu} B_\nu, \tag{7}$$

$$W(x, t) = \int_{-1}^{1} \left[\int_0^\infty I_\nu d\nu \right] \mu d\mu,$$

$$\rho c \frac{\partial T}{\partial t} = -\frac{\partial w}{\partial x} + \frac{\partial}{\partial x}\left[k \frac{\partial T}{\partial x} \right],$$

$\kappa_\nu = \kappa_{s\nu} + \kappa_{a\nu}$. We construct the solution in the domain $R = \{0 \leqq x \leqq H,\ 0 \leqq t \leqq t_M\}$ for the following boundary and initial conditions:

$$I_\nu(0, \mu, t) = B_\nu[T(0, t)], \quad \mu > 0; \quad I_\nu(H, \mu, t) = B_\nu[T_w(t)], \quad \mu < 0; \tag{8}$$

$$\frac{\partial T}{\partial x}(0, t) = 0; \ T(H, t) = T_w(t); \ T(x, 0) = T^0(x), \tag{9}$$

where $T_w(t)$ and $T^0(x)$ are given functions.

We solve the radiative transport equation numerically by the method of discrete ordinates, similar to that used in [6]. We rewrite the equation for the transport of $J_\nu = I_\nu - B_\nu$ along the direction $\mu = \mu_i$, $1 \leqq i \leqq N$, in the form

$$\mu_i \frac{\partial J_\nu^i}{\partial x} + \varkappa_\nu J_\nu^i = \frac{\varkappa_{s\nu}}{2} \sum_{n=1}^{N} a_n J_\nu^n - \mu_i \frac{\partial B_\nu}{\partial x}, \tag{10}$$

where a_n and μ_i are the weights and nodes of the N-point Gaussian quadrature formula. We introduce the subdivision $0 = x_0 \leqq x_1 < \ldots < x_M = H$ and the notation $J^i(x_s) = J^i{}_s$, $B[T(x_s)] = B_s$, $\tau^i{}_s = \kappa \Delta x^i{}_s/\mu_i$.

$$\Delta x_s^i = \begin{cases} x_s - x_{s+1}, & \mu_i < 0, \\ x_s - x_{s-1}, & \mu_i > 0, \end{cases}$$

and omit the subscript ν for brevity. The integration of (10) along the segment $\Delta x^i{}_s$, under the condition that $\partial B_\nu/\partial x$ depends only on T and ν on this segment, gives for $\mu_i \neq 0$:

$$J_s^i = J_{s+\delta}^i \Delta_s^i + \frac{1-\Delta_s^i}{\tau_s^i}\left[\frac{\tau_p^i}{2}\sum_{k=1}^{N} a_n J_s^n + B_{s+\delta} - B_s\right], \tag{11}$$

$$\delta = -\operatorname{sign}\mu_i, \quad \Delta_s^i = \exp(-\tau_s^i).$$

For $\mu_i = 0$ we have from Eq. (10)

$$J_s^i = \frac{\varkappa_s}{2\varkappa}\sum_{n=1}^{N} a_n J_s^n . \tag{12}$$

Boundary conditions (8) take the form

$$J_M^i = 0, \quad \mu_i < 0; \; J_0^i = 0, \; \mu_i > 0.$$

To take account of the spectral dependence of the radiation we divide the frequency range into the intervals $0 = \nu_0 < \nu_1 < \ldots < \nu_R < \infty$ and assume that in each interval $\Lambda_\ell = (\nu_{\ell-1}, \nu_\ell)$ the optical coefficients are independent of frequency. By integrating (11) and (12) with respect to frequency over Λ_ℓ, we obtain

$$\frac{\varkappa_s^l}{2\varkappa^l}\sum_{n=1}^{N} a_n J_s^{nl}, \quad \mu_i = 0, \tag{13}$$

$$J_{s+\delta}^{il}\Delta^{il} + \frac{1-\Delta^{il}}{\tau_s^{il}}\left[\frac{\tau_p^{il}}{2}\sum_{n=1}^{N} a_n J_s^{nl} + P_{s+\delta}^l - P_s^l\right], \quad \mu_i \neq 0,$$

where

$$J_s^{il} = \int_{\Lambda_l} J_s^i d\nu, \quad \tau_s^{il} = \int_{\Lambda_l} \tau_s^i d\nu, \quad P_s = 2\sigma T_s^4 \alpha_s^l,$$

$$\alpha_s^l = \frac{15}{\pi^4}\int_{z_s^{l-1}}^{z_s^l} \frac{x^3 dx}{\exp(x)-1}, \quad z_s^l = h\nu_l/kT_s, \quad \sigma = 5.67\cdot 10^{-5}\ \mathrm{g/cm^3deg^4}.$$

We calculate the heat fluxes with the formula

$$W_s = \sum_{n=1}^{N} a_n \mu_n \sum_{l=1}^{R} J_s^{nl}. \tag{14}$$

We solve system (13) by the Seidel iterative method, and stop the iterations when $\max_s |W_s - \tilde{W}_s| < \varepsilon \max_s |W_s|$, where $\tilde{W}_s$ is the value of W_s in the preceding iteration, $\varepsilon = 10^{-4}$.

As an initial approximation, we take the distribution of $J^{i\ell}{}_s$ in the preceding time step.

We approximate the heat-conduction equation by an implicit scheme, and use the pivotal method to solve the resulting linear algebraic system with a tridiagonal matrix.

2°. In the radiative heat-conduction approximation we describe the temperature distribution inside the sample by the equation

$$\rho c\frac{\partial T}{\partial t} = \frac{\partial}{\partial x_i}\left(k_i\frac{\partial T}{\partial x_i}\right), \tag{15}$$

where $k = (k_1, k_2, k_3)$ is the anisotropic variable thermal conductivity, including conductive and radiative components. The lateral and lower surfaces of the sample are assumed thermally insulated, $\partial T/\partial n = 0$. On the upper surface we specify the time dependence of either the temperature $T(t)|_{x=H} = T_W(t)$, or the heat flux. At time $t = 0$ the temperature of the sample is known. It is required to find the temperature of the lower surface of the sample. For a numerical solution we limit ourselves to a two-dimensional formulation of the problem with a scalar thermal conductivity $k_x = k_y = k$. We solve Eq. (15) by the method of variable directions, for which we write the following conservative longitudinal–transverse scheme [7]:

$$\frac{\bar{T}_{i,j}-T_{i,j}}{\tau/2}=\frac{2}{h_{i+1}+h_i}\left[\frac{\bar{T}_{i+1,j}\chi_{i+1,j}}{h_{i+1}}-\bar{T}_{i,j}\left(\frac{\chi_{i+1,j}}{h_{i+1}}+\frac{\chi_{i,j}}{h_i}\right)+\right.$$

$$\left.+\frac{\bar{T}_{i-1,j}\chi_{i,j}}{h_i}\right]+\frac{2}{l_{j+1}+l_j}\left[\frac{T_{i,j+1}\chi_{i,j+1}}{l_{j+1}}-T_{i,j}\left(\frac{\chi_{i,j+1}}{l_{j+1}}+\frac{\chi_{i,j}}{l_j}\right)+\frac{T_{i,j-1}\chi_{i,j}}{l_j}\right];$$

$$\frac{\hat{T}_{i,j}-\bar{T}_{i,j}}{\tau/2}=\frac{2}{h_{i+1}+h_i}\left[\frac{\bar{T}_{i+1,j}\chi_{i+1,j}}{h_{i+1}}-\bar{T}_{i,j}\left(\frac{\chi_{i+1,j}}{h_{i+1}}+\frac{\chi_{i,j}}{h_i}\right)+\right. \tag{16}$$

$$\left.+\frac{\bar{T}_{i-1,j}\chi_{i,j}}{h_i}\right]+\frac{2}{l_{j+1}+l_j}\left[\frac{\hat{T}_{i,j+1}\chi_{i,j+1}}{l_{j+1}}-\hat{T}_{i,j}\left(\frac{\chi_{i,j+1}}{l_{j+1}}+\frac{\chi_{i,j}}{l_j}\right)+\frac{\hat{T}_{i,j-1}\chi_{i,j}}{l_j}\right];$$

$$\chi_{i+1,j}=\frac{1}{2}[\chi(T_{i+1,j})+\chi(T_{i,j})];\ \chi_{i,j+1}=\frac{1}{2}[\chi(T_{i,j+1})+\chi(T_{i,j})].$$

Here h_i and ℓ_j are the mesh sizes in the x and y directions, and $T_{i,j} = T^n{}_{i,j}$, $\bar{T}_{i,j} = T^{n+\frac{1}{2}}{}_{i,j}$, $\hat{T}_{i,j} = T^{n+1}{}_{i,j}$, $\chi = k/\rho c$.

The effective thermal conductivity k was calculated as the sum of the thermal conductivity k_{cond} of a porous material and the radiative thermal conductivity k_{rad}

$$k = k_{cond} + k_{rad}. \tag{17}$$

Under the assumption of local thermodynamic equilibrium in the sample, we have [8]

$$k_{rad} = 16\sigma l T^3/3, \tag{18}$$

where ℓ is the average value of the Rosseland mean free path. In our case, ℓ is defined as $\ell = [\alpha\gamma(T)]^{-1}$. Here $\gamma(T)$ is the absorption coefficient for the radiation, and α is a numerical factor which from now on is found from a comparison with more accurate calculations with the preceding model (7)-(9).

3. Effective Model of Radiative Heat Conduction. We performed parallel numerical calculations by the two methods described above for the following parameters: L = 6 cm, H = 1-6 cm, $\rho_{mater} = 2.2$ g/cm³, porosity of sample P = 0.97, which corresponds to $\rho = \rho_{mater}(1 - P) = 0.066$ g/cm³, c = 729 J/kg·K, $k_{mater} = 1.36$ W/m·K. In accordance with [9, 10], $k_{cond} = k_{mater}c^2{}_p = 1.44\cdot 10^3$ cm/sec·K, where $c_p = 0.103$ is the unit cell parameter of the material, determined from its porosity. It should be noted that the thermal conductivity model used takes account of the actual structure of the material.

The first calculations were performed for the temperature dependence of the scattering coefficient $\kappa^0{}_s(T)$ given in Table 1, which is based on data in [9, 10]. It was assumed that for dispersed materials in which a characteristic dimension of the pores is appreciably larger than the wavelength of the radiation, the absorption and scattering coefficients are usually calculated for a single scatterer, and then the result is multiplied by the number of scatterers per unit volume.

It should be noted that this method of determining the coefficients is approximate. Therefore, these coefficients can be considered as the first approximation for the construction of a mathematical model. It is known that the absorption coefficient for visible light is much smaller than the scattering coefficient. Since we did not have more accurate information, we assumed that $\kappa_a = 10^{-2}\kappa_s$. We assumed that all the optical coefficients are independent of frequency and that the scattering is isotropic $[g_\nu(\mu, \mu') \equiv 1]$.

Figure 2 shows the time dependence of the temperature of the upper wall (curve 1) and that of the lower wall for various sample thicknesses (curves 2-4) calculated with the radiative

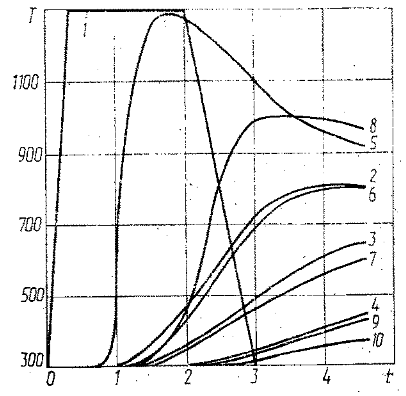

Fig. 2

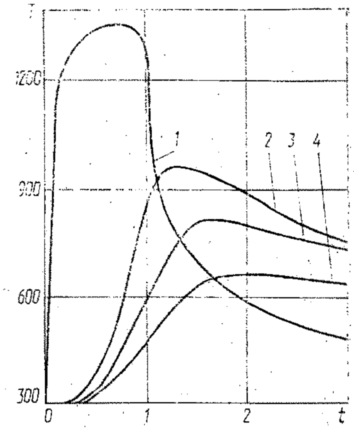

Fig. 3

Fig. 2. Time dependence of the temperature in the radiative-conductive heat transfer problem: 1) $T_w(t)$ of the upper wall; temperature of the lower wall calculated with the radiative heat transport model with: 2) H = 2 cm, 3) H = 2.5 cm, 4) H = 3 cm; 5, 6, 7) calculated in the radiative heat conduction approximation with H = 2 cm; 8, 9, 10) H = 3 cm; 5, 8) $\alpha = 0.1$; 6, 9) $\alpha = 4$; 7, 10) $\alpha = 1$. T is in °K and t in min.

Fig. 3. Results of calculations in the "gray material" approximation with the function $T_w(t)$ (curve 1) for $\kappa_a = 0.01\kappa^0_s$ (curve 2), $\kappa_a = \kappa^0_s$ (curve 3), and without taking account of radiative heat transfer (curve 4).

TABLE 1. Scattering Coefficient of Sample Material

T, °C	200	300	400	500	600	700	800
$\varkappa_s$, cm^{-1}	480—630	130—170	90—120	77—100	73—97	70—95	70—95
$\varkappa^0_s$, cm^{-1}	500	150	105	95	85	80	80

transport model. For H = 4 cm there is practically no heating of the lower wall. A decrease of the sample thickness naturally leads to stronger heating of the lower wall and to a shift of the temperature maximum to the left along the t axis. Calculations with different spatial nets (M = 10 and 20) gave nearly the same results. The maximum differences (about 10%) occurred at small values of t near x = H. On the surface x = 0 the differences did not exceed 2-3%. In view of this, subsequent calculations with the first model were performed with 10 nodes.

Curves 5-10 in Fig. 2 show the time dependence of the temperature of the lower surface of the sample calculated under these same conditions with the radiative heat conduction model with various values of α. In this formulation the problem is one-dimensional. It was solved on uniform 5 × 21 and 5 × 41 nets. Curves 5-7 correspond to H = 2 cm, and curves 8-10 to H = 3 cm. With a decrease of α, i.e., with an increase of the effective mean free path, the temperature of the lower surface of the sample increases markedly, and the maximum temperature is displaced toward the left. The results of the calculations with the radiative heat conduction model are in good agreement with analogous results calculated with the radiative transport model for a corresponding choice of α. For this formulation of the problem $\alpha = \alpha_0 = 0.4$. For samples of different thickness not only the magnitude, but also the position of the maximum of the temperature curve agree within 1-10%. Thus, by comparing these calculations we can construct an effective model of radiative heat conduction.

It should be noted that α can be chosen in this way only for parallel calculations with the two models. The value of α depends strongly on the heating conditions, and cannot be assumed to depend only on the material. At the same time, obtaining such a value of α for several different versions by comparing the results calculated with the two models is very useful for mathematical modeling in formulations more complicated than one-dimensional. For example, such a model can be effectively used to study combined heat transfer when the contribution of the convective component cannot be neglected. In order to describe the phenomenon in this case it is necessary to use Eqs. (1)-(3) with a thermal conductivity changed on the basis of the value of α obtained in this way.

4. Refinement of the Radiative Transport Model. The results of the next series of calculations are compared in more detail with experimental data for a specific sample of thickness H = 1 cm. The temperature of the upper surface was specified by the function $T_w(t)$ found from experiment and shown by curve 1 of Fig. 3. Curves 2-4 in this figure show T(0, t) for various versions of the calculation.

The calculation of radiative heat transport is made difficult by the lack of reliable data on the spectral optical coefficients. For our purposes the rather accurate data on the optical properties of quartz glass in [11] are very approximate, since they do not take account of the disperse structure of the material. This structure can turn out to be very important for determining the optical properties, since the characteristic dimensions of the structure of the material (2-10 μm) are comparable with the wavelength of the thermal radiation. In view of this, the data in [11] can be used only as an initial approximation for constructing a model to describe radiative heat transport.

The first calculations, like the preceding series, were performed in the "gray material" approximation. One purpose of the calculations was to find the importance of the contribution of radiative heat transport to the total heat transfer in the sample. This calculation gave a maximum temperature of 970°K, which is 300°K higher than in calculations which neglect radiation. An increase in absorption by a factor of 100 lowers the temperature somewhat, but it remained appreciably higher than in the calculations which neglected radiation. This shows that radiative heat transfer makes the predominant contribution to energy transport in the system under consideration, which shows the necessity of a more detailed account of this mechanism.

In order to construct a model of radiative transport in this medium, we again turn to the data in [11]. The characteristic form of the dependence of the absorption coefficient on wavelength is the following: for 0.3 μm < λ < 4.5 μm the material is practically transparent ($\kappa_a \sim 10^{-3}$ cm^{-1}), and outside this range the absorption coefficient increases by several orders of magnitude. At the temperatures of the present problem ($T \lesssim 0.1$ eV) there is practically no radiative transport in the range λ < 0.3 μm. For λ > 5 μm the variations of κ_a are rather large, but they occur against a background of $\kappa_a \approx 50$ cm^{-1}, i.e., the material is practically opaque. A previous test of the mathematical modeling of problems of the dynamics of a radiating gas justifies the use of the following two-group approximation in solving the radiative transport equation:

$$\varkappa_{a\nu} = \begin{cases} \varkappa_a^{\mathrm{I}}, & \lambda < 4.8\ \mu\mathrm{m}, \\ \varkappa_a^{\mathrm{II}}, & \lambda > 4.8\ \mu\mathrm{m}. \end{cases} \quad (19)$$

Although this approximation is very rough, it should represent the course of the process better than the "gray material" approximation. There is no point in introducing a large number of spectral groups in view of the lack of more detailed information on the optical coefficients.

Let us consider how the temperature distribution changes with a change of the optical properties in the two-group model. This series of calculations was performed simultaneously with an experimental study for a sample of thickness H = 1 cm in order to choose a final mathematical model.

Radiative transport calculated in the two-group approximation with $\kappa^{\mathrm{I}}_s = \kappa^0_s$. $\kappa^{\mathrm{II}}_a = 0.01\kappa^0_s$, $\kappa^{\mathrm{II}}_s = 0$, $\kappa^{\mathrm{II}}_a = 30$ cm^{-1} leads to the value T' = 429°, where T' is the deviation of the temperature of the lower wall at the time t = 1.7 min from its initial value. The lack of reliable data on the optical coefficients necessitates varying them over wide limits. Calculations showed that the optical properties of the material have a very strong effect on heat transport in the sample (Fig. 4). Thus, tripling the value of κ^{I}_s lowers the temperature T' to 320°, and increasing κ^{I}_s by a factor of five decreases T' to 295°. A further increase in scattering has practically no effect. Setting $\kappa^{\mathrm{II}}_a = 50$ cm^{-1} lowers T' at once to 240°. Setting $\kappa^{\mathrm{II}}_a = 50$ cm^{-1} and $\kappa^{\mathrm{I}}_s = 5\kappa^0_s$ simultaneously gives T' = 220°. In general, an increase of κ^{II}_a decreases T' more strongly than a change of other optical coefficients.

It is known [11] that κ^{I}_a should increase with an increase in temperature. By setting $\kappa^{\mathrm{I}} = 0.01\kappa^0_s$, we thus assume that κ^0_a is a decreasing function of the temperature, which is

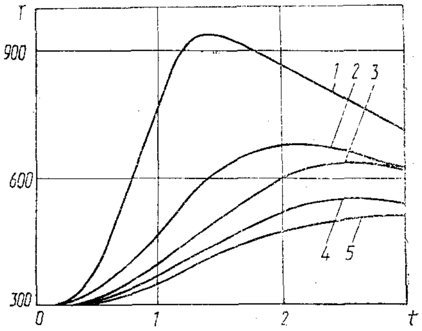

Fig. 4. Results of calculations in the two-group approximation: 1) $\kappa^I_s = \kappa^0_s$, $\kappa^I_a = 0.1\kappa^0_s$, $\kappa^{II}_a = 20\ cm^{-1}$; 2) $\kappa^I_s = 3\kappa^0_s$, $\kappa^I_a = 0.1\kappa^0_s$, $\kappa^{II}_a = 30\ cm^{-1}$; 3) $\kappa^I_s = 3\kappa^0_s$, $\kappa^I_a = 0.1\kappa^0_s$, $\kappa^{II}_a = 50\ cm^{-1}$; 4) $\kappa^I_s = 3\kappa^0_s$, $\kappa^I_a = 0.006\kappa^0_s$, $\kappa^{II}_a = 70\ cm^{-1}$; 5) $\kappa^I_s = 3\kappa^0_s$, $\kappa^I_a = 0.01\kappa^0_s$, $\kappa^{II}_a = 100\ cm^{-1}$.

certainly not true. In view of this, we assumed that the absorption coefficient in the short-wave region of the spectrum is given by the formula

$$\varkappa^I_a = 50 + 10^{-4}(T(K) - 300)^2\ (m^{-1}). \tag{20}$$

This choice of the temperature dependence of κ^I_a is determined by the overall regularities of the increase of the absorption coefficient with increasing temperature. Calculation with this κ^I_a and $\kappa^I_s = \kappa^0_s$, $\kappa^{II}_a = 70\ cm^{-1}$ gives T' = 250°.

The position of the boundary between the two spectral groups turns out to be very important. Thus, calculations showed that the displacement of the opacity boundary from $\lambda = 4.8$ µm to $\lambda = 2$ µm increases the temperature of the lower wall by 130-170° in various versions. Thus, it is clear that the radiative transport model employed has a substantial effect on the calculated results. Moreover, data obtained in various versions may turn out to be useful in designing future thermal insulation coatings, since at the same time the temperature dependence of the optical properties of the material is traced.

However, in order to choose a radiative transport model which adequately describes heat transfer for a specific thermal insulation material, it is necessary to know the relation between numerical and full-scale experiments. The latter shows that for the sample under consideratin T' = 150°. On the other hand, a numerical experiment shows that a variation of κ^{II}_a affects the temperature change most strongly. Variations of the scattering coefficient, particularly for $\kappa_s \geqq 3\kappa^0_s$, have a much smaller effect on the temperature. Assuming that κ^I_a is detrmined with Eq. (20), $\kappa^I_s = 3\kappa^0_s$, we find which κ^{II}_s to choose in order to match data of full-scale and numerical experiments. This absorption coefficient for the second group turned out to be $\kappa^{II}_a = 70\ cm^{-1}$. With this choice of optical properties there is good agreement of the calculated and experimental alues of the temperature at all times.

Of course, a final choice of a transport model requires a comparison with data from a large number of experiments. However, the construction of a mathematical model of radiative transport in thermal insulation materials should surely be based on the study of data from a full-scale experiment. Clearly, other thermophysical properties of dispersed materials can also be determined in this way.

NOTATION

$\bar{V}$, velocity; ρ, density; p, pressure; T, temperature of medium; K, filtration tensor; ν, χ, β, effective kinematic viscosity, thermal diffusivity, and coefficient of thermal expansion; g, acceleration produced by external forces; H × L, dimensions of sample; ω, curl of the velocity; ψ, stream function; $I_\nu(x, \mu, t)$, spectral intensity of radiation; μ, cosine of angle between the x axis and the path of a photon; $B_\nu(T)$, Planck function; W, radiant energy flux density; $g_\nu(\mu, \mu')$, scattering indicatrix; c(T), k(T), specific heat and thermal conductivity of material; $\kappa_{s\nu}$, $\kappa_{a\nu}$, spectral scattering and absorption coefficients; λ, wavelength of radiation.

LITERATURE CITED

1. A. A. Samarskii, "Mathematical modeling and numerical experiment," Vestn. Akad. Nauk SSSR, No. 5, 38-48 (1979).
2. A. A. Samarskii, "Numerical methods of solving multidimensional problems of mechanics and physics," Zh. Vychsl. Mat. Mat. Fiz., 20, 1416-1464 (1980).
3. V. I. Aravin and S. N. Numerov, Theory of Motion of Liquids and Gases in Undeformed Porous Media [in Russian], Gostekhizdat, Moscow (1953).

4. B. P. Gerasimov, T. G. Elizarova, and V. I. Turchaninov, "The method of suppression of network viscosity in the solution of the Navier–Stokes equations," Differents. Uravn., No. 7, 1165-1173 (1984).
5. A.A. Samarskii, "Contemporary applied mathematics and numerical experiment," Kommunist, No. 18, 31-42 (1983).
6. E. V. Shil'nikov, "Calculation of the effect of laser radiation on gaseous carbon," in: Dynamics of a Radiating Gas [in Russian], No. 3, Computing Center, Academy of Sciences of the USSR, Moscow (1980), pp. 25-32.
7. A. A. Samarskii, Theory of Difference Schemes [in Russian], Nauka, Moscow (1977).
8. Ya. B. Zel'dovich and Yu. P. Raizer, Physics of Shock Waves and High-Temperature Hydrodynamic Phenomena, Academic Press, New York (1966).
9. E. Ya. Litovskii and N. A. Puchkevich, Thermophysical Properties of Refractory Materials [in Russian], Metallurgiya, Moscow (1982).
10. G. N. Dul'nev and Yu. P. Zarichnyak, Thermal Conductivity of Mixtures and Composite Materials [in Russian], Énergiya, Leningrad (1974).
11. V. A. Petrov, "Optical properties of quartz glasses at high temperatures in the region of their semitransparency," in: Compilations of Thermophysical Properties of Materials, No. 3(17) [in Russian], Institute of High Temperatures, Academy of Sciences of the USSR, Moscow (1979), pp. 29-72.

NUMERICAL-ANALYTICAL MODELING OF HEAT TRANSFER BETWEEN A LAMINAR FLOW AND HIGHLY PERMEABLE ROUGHNESS

Ya. Ya. Karchev and E. A. Gaev

UDC 532.517.2:536.24

A mathematical model is proposed for the thermal interaction of a laminar flow with a layer of small stationary streamlined obstacles. Numerical and analytical investigations exhibit characteristic zones of the flow.

A concept that has proved useful for the solution of a number of practical problems [1-4] is the notion of highly permeable roughness (HPR), which we interpret in the present study as a plane layer $0 \leqq x < \infty$, $0 \leqq z \leqq h$ randomly filled with stationary streamlined obstacles. We assume for definiteness that the obstacles are nondeformable spheres of diameter d, which is much smaller than the thickness h of the HPR. Their concentration is small enough that hydrodynamic and thermal interaction does not take place between them.

Let an unbounded viscous fluid flow with temperature-independent properties move along the HPR. The intensity of interaction of the flow with the HPR is determined by the local velocity U(z) of the flow relative to the obstacles, the local temperature difference $\Theta - \vartheta$ between the fluid and the obstacles, and the concentration (number density) n of the obstacles per unit volume. Owing to the smallness of the concentration, $\partial p/\partial z = 0$. A mathematical model of the flow produced by the HPR can be written in the form of boundary-layer equations with source terms. The latter have a discontinuity at the line of demarcation between the hindered and external flows, z = h [1, 2]:

$$f=\begin{cases}\rho knU,\\ 0,\end{cases}\qquad i=\begin{cases}\alpha n(\Theta-\vartheta)S, & 0\leqslant z\leqslant h,\\ 0, & z>h.\end{cases}\tag{1}$$

The drag coefficient k (m^3/sec) of the obstacles is assumed to be constant. For small Reynolds numbers $Re' = U_\infty d/\nu < 1$, e.g., $k = 3\pi\nu d$ (Stokes' law). Analogously, α = const and does not depend on the flow velocity. The hydrodynamic interaction of a flow with HPR has been investigated in our previous work. Here we turn our attention to the heat-transfer problem.

V. Ya. Chubar' Mechanical Engineering Institute, Zaporozhe. Translated from Inzhenerno-Fizicheskii Zhurnal, Vol. 49, No. 5, pp. 791-797, November, 1985. Original article submitted October 22, 1984.

 0022-0841/85/4905-1314$09.50